

AperTO - Archivio Istituzionale Open Access dell'Università di Torino

Tracking dynamics of magma migration in open-conduit systems

This is a pre print version of the following article:

Original Citation:

Availability:

This version is available <http://hdl.handle.net/2318/1615081> since 2019-05-08T10:10:06Z

Published version:

DOI:10.1007/s00445-016-1072-x

Terms of use:

Open Access

Anyone can freely access the full text of works made available as "Open Access". Works made available under a Creative Commons license can be used according to the terms and conditions of said license. Use of all other works requires consent of the right holder (author or publisher) if not exempted from copyright protection by the applicable law.

(Article begins on next page)

Dear Author

Here are the proofs of your article.

- You can submit your corrections **online**, via **e-mail** or by **fax**.
- For **online** submission please insert your corrections in the online correction form. Always indicate the line number to which the correction refers.
- You can also insert your corrections in the proof PDF and **email** the annotated PDF.
- For **fax** submission, please ensure that your corrections are clearly legible. Use a fine black pen and write the correction in the margin, not too close to the edge of the page.
- Remember to note the **journal title**, **article number**, and **your name** when sending your response via e-mail or fax.
- **Check** the metadata sheet to make sure that the header information, especially author names and the corresponding affiliations are correctly shown.
- **Check** the questions that may have arisen during copy editing and insert your answers/corrections.
- **Check** that the text is complete and that all figures, tables and their legends are included. Also check the accuracy of special characters, equations, and electronic supplementary material if applicable. If necessary refer to the *Edited manuscript*.
- The publication of inaccurate data such as dosages and units can have serious consequences. Please take particular care that all such details are correct.
- Please **do not** make changes that involve only matters of style. We have generally introduced forms that follow the journal's style.
- Substantial changes in content, e.g., new results, corrected values, title and authorship are not allowed without the approval of the responsible editor. In such a case, please contact the Editorial Office and return his/her consent together with the proof.
- If we do not receive your corrections **within 48 hours**, we will send you a reminder.
- Your article will be published **Online First** approximately one week after receipt of your corrected proofs. This is the **official first publication** citable with the DOI. **Further changes are, therefore, not possible.**
- The **printed version** will follow in a forthcoming issue.

Please note

After online publication, subscribers (personal/institutional) to this journal will have access to the complete article via the DOI using the URL:

<http://dx.doi.org/10.1007/s00445-016-1072-x>

If you would like to know when your article has been published online, take advantage of our free alert service. For registration and further information, go to:

<http://www.link.springer.com>.

Due to the electronic nature of the procedure, the manuscript and the original figures will only be returned to you on special request. When you return your corrections, please inform us, if you would like to have these documents returned.

Metadata of the article that will be visualized in OnlineFirst

1	Article Title	Tracking dynamics of magma migration in open-conduit systems	
2	Article Sub- Title		
3	Article Copyright - Year	Springer-Verlag Berlin Heidelberg 2016 (This will be the copyright line in the final PDF)	
4	Journal Name	Bulletin of Volcanology	
5		Family Name	Valade
6		Particle	
7		Given Name	Sebastien
8	Corresponding	Suffix	
9	Author	Organization	Università di Firenze
10		Division	Dipartimento di Scienze della Terra
11		Address	Florence
12		e-mail	valade.sebastien@gmail.com
13		Family Name	Lacanna
14		Particle	
15		Given Name	Giorgio
16	Author	Suffix	
17		Organization	Università di Firenze
18		Division	Dipartimento di Scienze della Terra
19		Address	Florence
20		e-mail	
21		Family Name	Coppola
22		Particle	
23		Given Name	Diego
24	Author	Suffix	
25		Organization	Università di Torino
26		Division	Dipartimento di Scienze della Terra
27		Address	Turin
28		e-mail	
29		Family Name	Laiolo
30	Author	Particle	
31		Given Name	Marco

32		Suffix	
33		Organization	Università di Torino
34		Division	Dipartimento di Scienze della Terra
35		Address	Turin
36		e-mail	
37		Family Name	Pistolesi
38		Particle	
39		Given Name	Marco
40	Author	Suffix	
41		Organization	Università di Firenze
42		Division	Dipartimento di Scienze della Terra
43		Address	Florence
44		e-mail	
45		Family Name	Donne
46		Particle	
47		Given Name	Dario Delle
48	Author	Suffix	
49		Organization	Università di Palermo
50		Division	Dipartimento di Scienze della Terra e del Mare
51		Address	Palermo
52		e-mail	
53		Family Name	Genco
54		Particle	
55		Given Name	Riccardo
56	Author	Suffix	
57		Organization	Università di Firenze
58		Division	Dipartimento di Scienze della Terra
59		Address	Florence
60		e-mail	
61		Family Name	Marchetti
62		Particle	
63		Given Name	Emanuele
64	Author	Suffix	
65		Organization	Università di Firenze
66		Division	Dipartimento di Scienze della Terra
67		Address	Florence
68		e-mail	

69		Family Name	Ulivieri
70		Particle	
71		Given Name	Giacomo
72	Author	Suffix	
73		Organization	Università di Firenze
74		Division	Dipartimento di Scienze della Terra
75		Address	Florence
76		e-mail	
<hr/>			
77		Family Name	Allocca
78		Particle	
79		Given Name	Carmine
80	Author	Suffix	
81		Organization	Università di Firenze
82		Division	Dipartimento di Scienze della Terra
83		Address	Florence
84		e-mail	
<hr/>			
85		Family Name	Cigolini
86		Particle	
87		Given Name	Corrado
88	Author	Suffix	
89		Organization	Università di Torino
90		Division	Dipartimento di Scienze della Terra
91		Address	Turin
92		e-mail	
<hr/>			
93		Family Name	Nishimura
94		Particle	
95		Given Name	Takeshi
96	Author	Suffix	
97		Organization	Tohoku University
98		Division	Department of Geophysics
99		Address	Sendai
100		e-mail	
<hr/>			
101		Family Name	Poggi
102		Particle	
103	Author	Given Name	Pasquale
104		Suffix	
105		Organization	Istituto Nazionale di Ottica-CNR

106		Division	
107		Address	Florence
108		e-mail	
109		Family Name	Ripepe
110		Particle	
111		Given Name	Maurizio
112	Author	Suffix	
113		Organization	Università di Firenze
114		Division	Dipartimento di Scienze della Terra
115		Address	Florence
116		e-mail	
117		Received	30 March 2016
118	Schedule	Revised	
119		Accepted	26 September 2016
120	Abstract	<p>Open-conduit volcanic systems are typically characterized by unsealed volcanic conduits feeding permanent or quasi-permanent volcanic activity. This persistent activity limits our ability to read changes in the monitored parameters, making the assessment of possible eruptive crises more difficult. We show how an integrated approach to monitoring can solve this problem, opening a new way to data interpretation. The increasing rate of explosive transients, tremor amplitude, thermal emissions of ejected tephra, and rise of the very-long-period (VLP) seismic source towards the surface are interpreted as indicating an upward migration of the magma column in response to an increased magma input rate. During the 2014 flank eruption of Stromboli, this magma input preceded the effusive eruption by several months. When the new lateral effusive vent opened on the Sciara del Fuoco slope, the effusion was accompanied by a large ground deflation, a deepening of the VLP seismic source, and the cessation of summit explosive activity. Such observations suggest the drainage of a superficial magma reservoir confined between the crater terrace and the effusive vent. We show how this model successfully reproduces the measured rate of effusion, the observed rate of ground deflation, and the deepening of the VLP seismic source. This study also demonstrates the ability of the geophysical network to detect superficial magma recharge within an open-conduit system and to track magma drainage during the effusive crisis, with a great impact on hazard assessment.</p>	
121	Keywords separated by ' - '	Magma - Open-conduit system - Volcano	
122	Foot note information	Editorial responsibility: M.R. Patrick	
		The online version of this article (doi:10.1007/s00445-016-1072-x) contains supplementary material, which is available to authorized	

users.

Electronic supplementary material

ESM 1

(MP4 23,146 kb)

1
3
2

RESEARCH ARTICLE

4

Tracking dynamics of magma migration in open-conduit systems

Q1 5
6
7
8
9

Sebastien Valade¹ · Giorgio Lacanna¹ · Diego Coppola² · Marco Laiolo² ·
Marco Pistolesi¹ · Dario Delle Donne³ · Riccardo Genco¹ · Emanuele Marchetti¹ ·
Giacomo Olivieri¹ · Carmine Allocca¹ · Corrado Cigolini² · Takeshi Nishimura⁴ ·
Pasquale Poggi⁵ · Maurizio Ripepe¹

10
11

Received: 30 March 2016 / Accepted: 26 September 2016
© Springer-Verlag Berlin Heidelberg 2016

12
13
14
15
16
17
18
19
20
21
22
23
24
25
26
27
28
29

Abstract Open-conduit volcanic systems are typically characterized by unsealed volcanic conduits feeding permanent or quasi-permanent volcanic activity. This persistent activity limits our ability to read changes in the monitored parameters, making the assessment of possible eruptive crises more difficult. We show how an integrated approach to monitoring can solve this problem, opening a new way to data interpretation. The increasing rate of explosive transients, tremor amplitude, thermal emissions of ejected tephra, and rise of the very-long-period (VLP) seismic source towards the surface are interpreted as indicating an upward migration of the magma column in response to an increased magma input rate. During the 2014 flank eruption of Stromboli, this magma input preceded the effusive eruption by several months. When the new lateral effusive vent opened on the Sciara del Fuoco slope, the effusion was accompanied by a large ground deflation, a deepening of the VLP seismic source, and the cessation of summit explosive activity. Such observations suggest the drainage of a

superficial magma reservoir confined between the crater terrace and the effusive vent. We show how this model successfully reproduces the measured rate of effusion, the observed rate of ground deflation, and the deepening of the VLP seismic source. This study also demonstrates the ability of the geophysical network to detect superficial magma recharge within an open-conduit system and to track magma drainage during the effusive crisis, with a great impact on hazard assessment. 30
31
32
33
34
35
36
37

Keywords Magma · Open-conduit system · Volcano 38 Q4

Introduction 39

Open-conduit volcanoes are characterized by persistent volcanic activity through unsealed volcanic conduits. This implies that such systems do not experience significant internal pressurization and consequently do not show significant long-term edifice deformation preceding volcanic eruptions (Chaussard et al. 2013). The forecasting of eruptive crises in open systems thus becomes difficult, because monitoring of ground deformation cannot be used to unequivocally identify episodes of new magma addition to magmatic reservoirs. 40
41
42
43
44
45
46
47
48

Stromboli volcano (Italy) is one of the most famous open-conduit basaltic systems. It is well-known for its persistent Strombolian explosive activity which has been ongoing for centuries (Rosi et al. 2000, 2013), characterized by rhythmic mild explosions ejecting lapilli, bombs, ash, and a minor lithic component from the active craters. During periods of ordinary activity, the average magma supply rate from depth is 0.1–0.5 m³/s (Allard et al. 1994; Harris and Stevenson 1997; Ripepe et al. 2005; Burton et al. 2007). This steady-state regime is sometimes interrupted by effusive crises, characterized by the opening of new lateral eruptive vents which feed cubic megameter-large, weeks- to months-duration lava flows 49
50
51
52
53
54
55
56
57 Q5
58
59
60

Editorial responsibility: M.R. Patrick

Electronic supplementary material The online version of this article (doi:10.1007/s00445-016-1072-x) contains supplementary material, which is available to authorized users.

Q2

✉ Sebastien Valade
valade.sebastien@gmail.com

Q3

¹ Dipartimento di Scienze della Terra, Università di Firenze, Florence, Italy
² Dipartimento di Scienze della Terra, Università di Torino, Turin, Italy
³ Dipartimento di Scienze della Terra e del Mare, Università di Palermo, Palermo, Italy
⁴ Department of Geophysics, Tohoku University, Sendai, Japan
⁵ Istituto Nazionale di Ottica-CNR, Florence, Italy

61 (Barberi et al. 1993, 2009; Marsella et al. 2011). These effu- 111
 62 sive eruptions have been in the past frequently associated with 112
 63 lateral tsunamogenic landslides occurring immediately before 113
 64 or during the first (hours to days) phases of the effusive erup- 114
 Q6 65 tion (Tinti et al. 2006; Chiocci et al. 2008). Moreover, the 115
 66 persistent activity can also be interrupted by more violent
 67 *major* explosions (~2 per year) with the formation of ash-
 68 and lapilli-charged plumes up to a few hundred meters high
 69 (Barberi et al. 1993; Rosi et al. 2013). More rarely (every 5–
 70 10 years), *paroxysmal* explosions forming plumes a few kilo-
 71 meters high can strike the villages with the fallout of pumice
 72 and ballistic blocks (Barberi et al. 1993; Rosi et al. 2013). Our
 73 ability to predict all of these events outside the range of the
 74 mild persistent Strombolian activity is intimately related to the
 75 capability of the monitoring network to track in real time the
 76 migration of magma towards the surface within the shallow
 77 portions of the edifice.

78 The 2014 effusive eruption, which lasted from August 7
 79 until November 22, was the most recent of four important
 80 events in the last 30 years (i.e., 1985, 2002–2003, 2007,
 81 and 2014; De Fino et al. 1988; Calvari et al. 2005, 2010;
 82 Barberi et al. 2009). We describe the 2014 eruption using
 83 data from a geophysical monitoring network including
 84 seismic, infrasonic, tilt, and thermal sensors, deployed
 85 and operated by the University of Firenze (UNIFI) since
 86 2003 (Ripepe et al. 2004). Additionally, we integrate lava
 87 discharge rate data retrieved from satellite thermal images
 88 (Coppola et al. 2013, 2015). In the present study, we demon-
 89 strate the ability of the network to detect the magma
 90 recharge and discharge processes in the shallow conduit
 91 system, as well as its ability to track the migration of mag-
 92 ma within the conduit system. We provide a quantitative
 93 model to explain the data collected during the effusive
 94 eruption as the discharge of a shallow reservoir, and we
 95 suggest an interpretative model of Stromboli's magma
 96 recharge/drainage cycles, eventually discussing the
 97 model's implications for hazard assessment.

98 **Monitoring geophysical network**

99 The monitoring network operated by the Laboratorio di
 100 Geofisica Sperimentale (LGS) of the UNIFI was deployed in
 101 January 2003, and it has been in continuous expansion ever
 Q7 102 since (Ripepe et al. 2004, 2005, 2007, 2009; Fig. 1a). It cur- 150
 103 rently consists of four seismo-acoustic stations (ROC, PZZ,
 104 STR, and SCI), one five-element infrasonic array (EAR), two
 105 thermal infrared cameras (ROC and GST), four tiltmeters
 106 (borehole: OHO, LSC, and LFS; surface: CPL), and one
 107 gauge for tsunami monitoring (PDC). All data are radio trans-
 108 mitted to the monitoring center of the Department of the Civil
 109 Protection (COA) on the island, where data are collected,
 110 processed, and published in real time on the Web. In addition,

thermal satellite remote sensing using the moderate-resolution 111
 imaging spectroradiometer (MODIS) sensor is achieved 112
 through MIROVA (Middle InfraRed Observation of 113
 Volcanic Activity), in collaboration with the University of 114
 Torino (Coppola et al. 2015). 115

116 **Geophysical evidence of magma recharge/discharge**
 117 **process**

118 The 2014 flank eruption provided high-quality geophysical 118
 119 data on processes occurring within the shallow feeding system 119
 of Stromboli. The eruptive crisis is hereafter described in three 120
 main phases: (1) the months-long pre-effusive recharging 121
 phase, characterized by the progressive increase in explosive 122
 activity at the summit craters; (2) the effusive onset, marked 123
 by a small lava flow originated from the partial collapse of the 124
 northeast 1 (NE1) crater on August 6, followed by the opening 125
 of a new lateral effusive vent on August 7; and (3) the weeks- 126
 long effusive discharging phase, characterized by a gradual 127
 decrease in the lava effusion rate. 128

129 **Pre-effusive phase: magma recharge**

130 Nearly 4 months prior to the eruption onset, most of the geo- 130
 131 physical parameters started to outline an escalation in the ex- 131
 132 plosive activity. The tremor amplitude gradually increased 132
 (Fig. 2(a)), along with the rate of very-long-period (VLP, 133
 10–20-s period) seismic activity (black curve in Fig. 2(b)). 134
 This trend was associated with the decrease of the VLP polar- 135Q8
 136 ization dip angle (blue curve in Fig. 2(b)), calculated as the 136
 137 angle between the main axis of the polarization vector of the 137
 138 VLP seismic source and the horizontal plane (Marchetti and 138
 139 Ripepe 2005; Ripepe et al. 2015) at station STR. Thus, the 139
 140 decrease of the polarization dip angle indicates a migration of 140
 141 the position of the VLP seismic source towards the surface. 141
 The acoustic pressure of the explosions also increased 142
 (Fig. 2(d)), together with thermal measurements from both 143
 144 ground- and satellite-based sensors (Fig. 2(e, f)), which indi- 144
 145 cate an increase in frequency and intensity (tephra volume and 145
 146 exit velocities) of the explosions, resulting in a larger amount 146
 147 of hot material emitted from the summit craters. Tephra vol- 147
 148 umes and exit velocities, in particular, are estimated by real- 148
 149 time processing of thermal camera data, as described in Delle 149
 150 Donne and Ripepe (2012). It is worth noting that this increase 150
 151 in the monitored parameters and explosive activity followed a 151
 152 local earthquake of moderate size ($M_L = 2.5$) at 6.2 km below 152
 153 the edifice on May 26, 2014 (INGV Centro Nazionale 153
 154 Terremoti). 154

155 During this period of increased activity, nine short-lived 155
 156 lava overflows were recorded (Fig. 2, orange stripes) from 156
 157 the active vents, which remain mostly confined within the 157
 158 crater terrace or in the upper part of the Sciara del Fuoco. 158

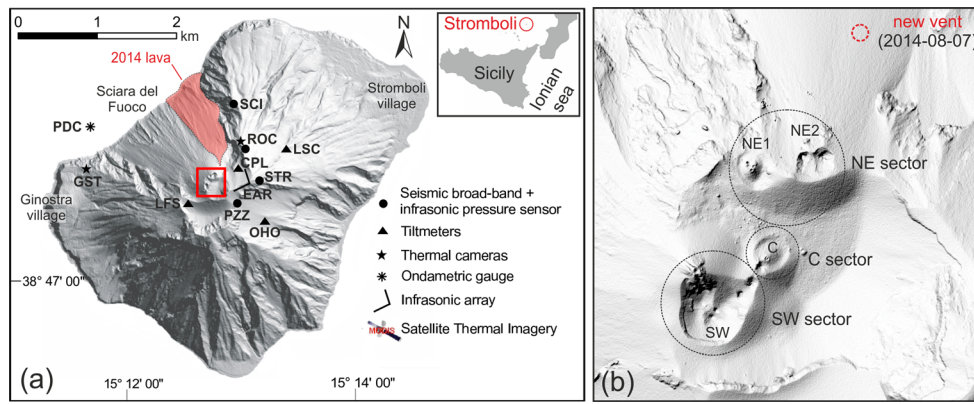


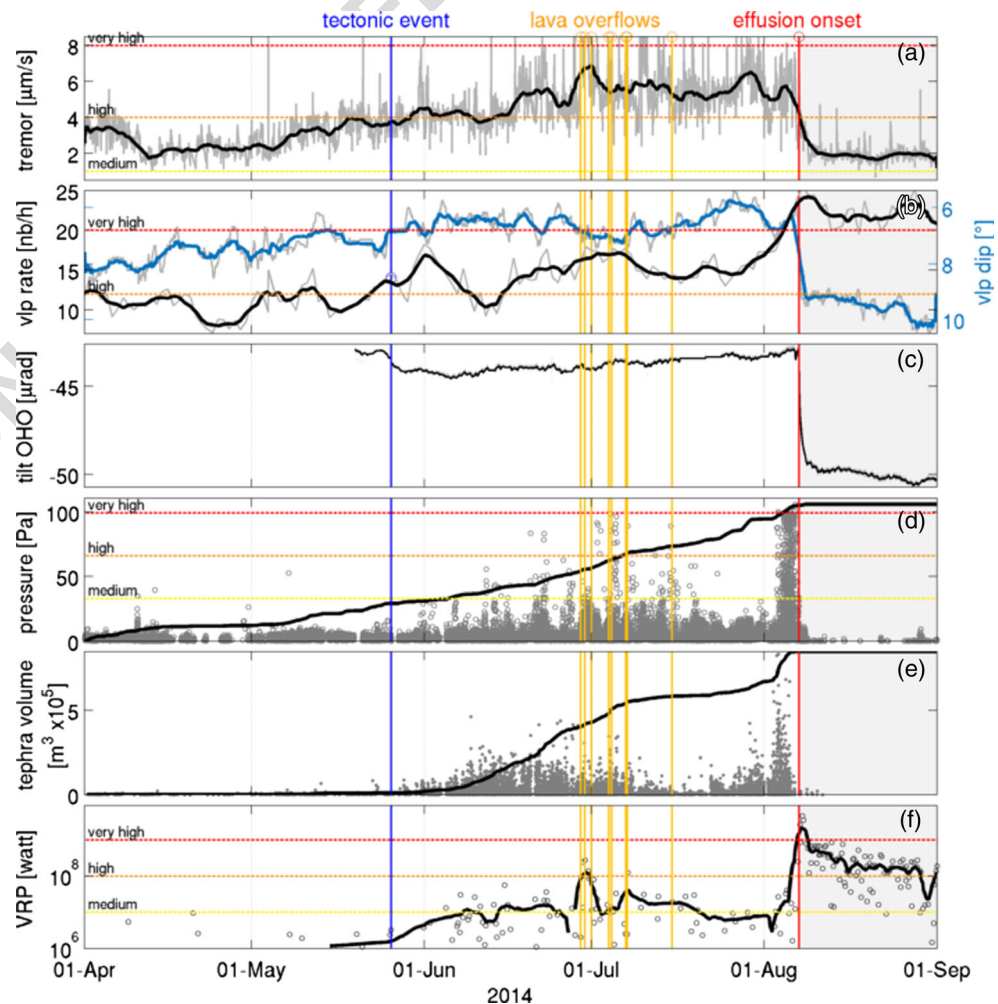
Fig. 1 Shaded relief map of the Stromboli volcano. **a** Location of the geophysical sensors and extent of the 2014 lava flow in red. **b** Location of the main craters (SW southwest crater, C central crater, NE1 northeast 1 crater, NE2 northeast 2 crater) and of the new eruptive vent opened on

August 7, 2014, which fed the lava flow. The digital elevation model computed from images taken in 2014 is courtesy of the Italian Civil Protection

159 Most overflows in 2014 were characterized by the same distinctive features: increasing spatter activity from the NE1 crater, accompanied by a rapid increase in both tremor amplitude (Fig. 3(a)) and infrasonic pressure (Fig. 3(b)), with no significant ground inflation. As the spattering activity reached the

164 maximum rate of 1–2 explosions/s, the infrasonic activity 165 shifted from the central crater towards the NE1 crater 166 (Fig. 3(d)). Simultaneously, when lava overflowed from the 167 crater onto the Sciara del Fuoco, all tiltmeters detected a clear 168 ground deflation, with an amplitude typically <0.2 μm at the

Fig. 2 Evolution of the geophysical parameters 4 months prior to the onset of effusion (April 1–August 7, 2014) and 1 month afterwards (August 7–September 1, 2014). The parameters highlight increasing explosive activity, evidenced by increasing seismic tremor (a), increasing rate and dip of VLP seismicity (black and blue curves, respectively) (b), increasing infrasonic pressures (d), and increasing tephra emissions from ground-based (e) and satellite-based (f) thermal sensor. The ground deformation (c) from borehole tiltmeter does not show large-scale ground inflation prior to the onset of effusion. The red vertical bar indicates the timing of the eruption onset, corresponding to the opening of the new effusive vent on August 7, 2014. The orange vertical bars indicate the timing of the overflow events and the blue vertical bar the timing of local earthquake recorded on May 26, 2014



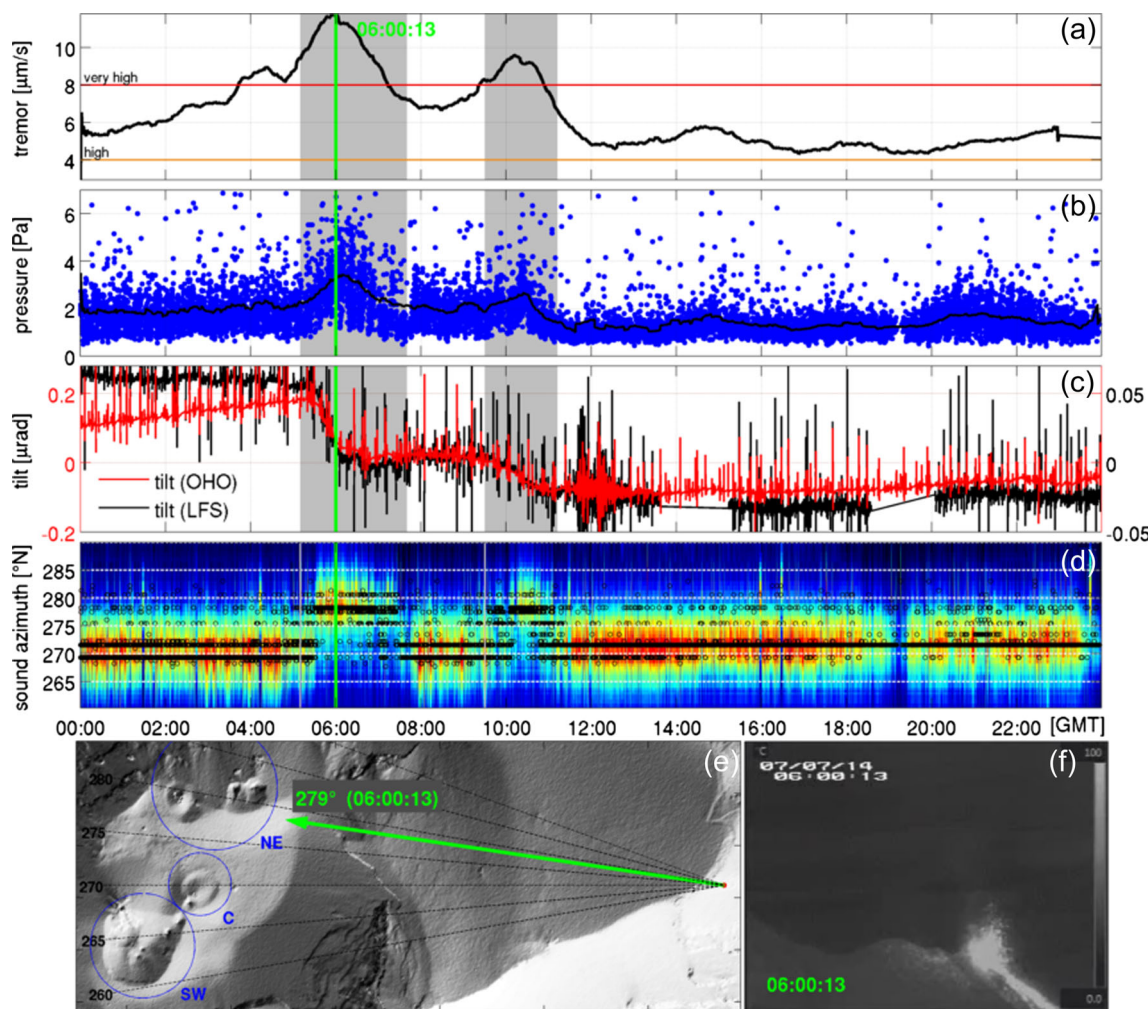


Fig. 3 Evolution of geophysical parameters during two overflow events (highlighted in gray) recorded on July 7, 2014: *a* seismic tremor, *b* infrasonic pressures, *c* ground deformation, *d* infrasonic sound azimuth, *e* projection of sound azimuth onto digital elevation model, and *f* snapshot

of the thermal infrared camera ROC as lava overflows from the NE1 crater onto the upper portion of the Sciara del Fuoco. The time of the snapshot is indicated by a green bar in the time series (*a–d*), and a green arrow in plot (*e*) indicates the corresponding infrasound azimuth

169 OHO station (Fig. 3(c), Supplementary Material), indicating
 170 the decompression of the magmatic system. Tremor amplitude
 171 and infrasonic pressure continued to increase during the de-
 172 compression until the maximum deflation was reached
 173 (Fig. 3). This possibly suggests that the overflow itself en-
 174 hances explosive/spattering activity by decompressing the
 175 magmatic system after the removal of the upper part of the
 176 magma column.

177 Three days prior to the eruption onset, on August 3, the
 178 explosive activity increased significantly, as shown by large
 179 infrasonic pressure, high VLP rate, and the amount of ejected
 180 tephra volumes (Fig. 2(b–e)).

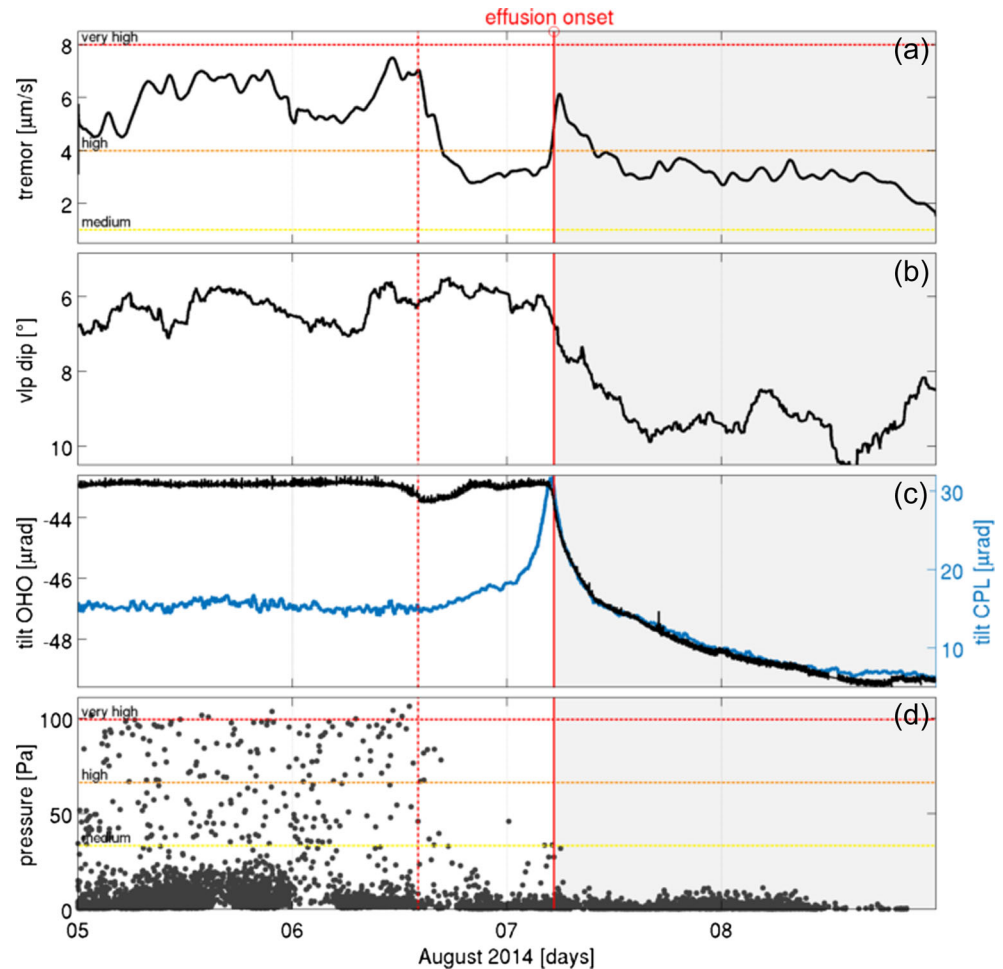
181 The simultaneous increase of all the monitored geophysical
 182 parameters suggests that an increase of the magma/gas input
 183 rate already started ~4 months prior to the effusive eruption
 184 onset, forcing the magma column towards the surface, as shown
 185 by the gradual upward migration of the VLP seismic source.

This lead to a progressive increase of the explosive activity and
 to the numerous overflows recorded during this period.

Effusive onset: vent opening

The onset of the effusive eruption is marked by the opening
 of a lateral effusive vent along the Sciara del Fuoco
 on August 7, 2014, at 05:00 GMT (solid red line in
 Fig. 4). However, the vent opening was preceded by a
 complex phase which lasted nearly 15 h. This phase ini-
 tiated with the collapse of a portion of the NE1 crater rim
 (dashed red line in Fig. 4), generating a large rockfall
 on the Sciara del Fuoco which was detected by all the sei-
 smic stations. This collapse initiated a small lava flow
 which reached the sea in a few hours. During this short-
 lived lava flow from the NE1 crater, the explosive activity
 decreased significantly, as indicated by the drop of the
 tremor amplitude, the rate, and the pressure of infrasonic

Fig. 4 Evolution of the geophysical parameters a few days prior to and after the onset of effusion. The *dashed vertical red bar* indicates the time when a portion of the NE1 crater collapsed and the onset of a small lava flow. Nearly 15 h afterwards, a new effusive vent opened (August 7, 2014 at 05:00 GMT) as indicated by the *solid red line*. During this time interval, ground inflation was recorded at the CPL tiltmeter, as well as a drop in the infrasonic pressures and volcanic tremor



202 transients (Fig. 4(a, d)). This drop is also accompanied by
 203 a short deflation of 0.52 μrad at the OHO tiltmeter (black
 204 curve in Fig. 4(c)). Moreover, during the 15 h following
 205 the collapse of the NE1 crater, the CPL tiltmeter recorded
 206 a progressive ground inflation of $\sim 13 \mu\text{rad}$ (blue curve in
 207 Fig. 4(c)), which culminated on August 7, 2014, at
 208 $\sim 05:00$ GMT with the opening of a new effusive vent
 209 on the lower parts of the NE2 crater flank at ~ 670 m
 210 above sea level (a.s.l.) (Fig. 1). The CPL tiltmeter, located
 211 200 m from the new effusive vent, is the only one to have
 212 recorded this phenomenon with such intensity, implying a
 213 very localized and shallow source, which is consistent
 214 with the intrusion of a very shallow lateral dyke from the
 215 main conduit towards the northern flank of the edifice.

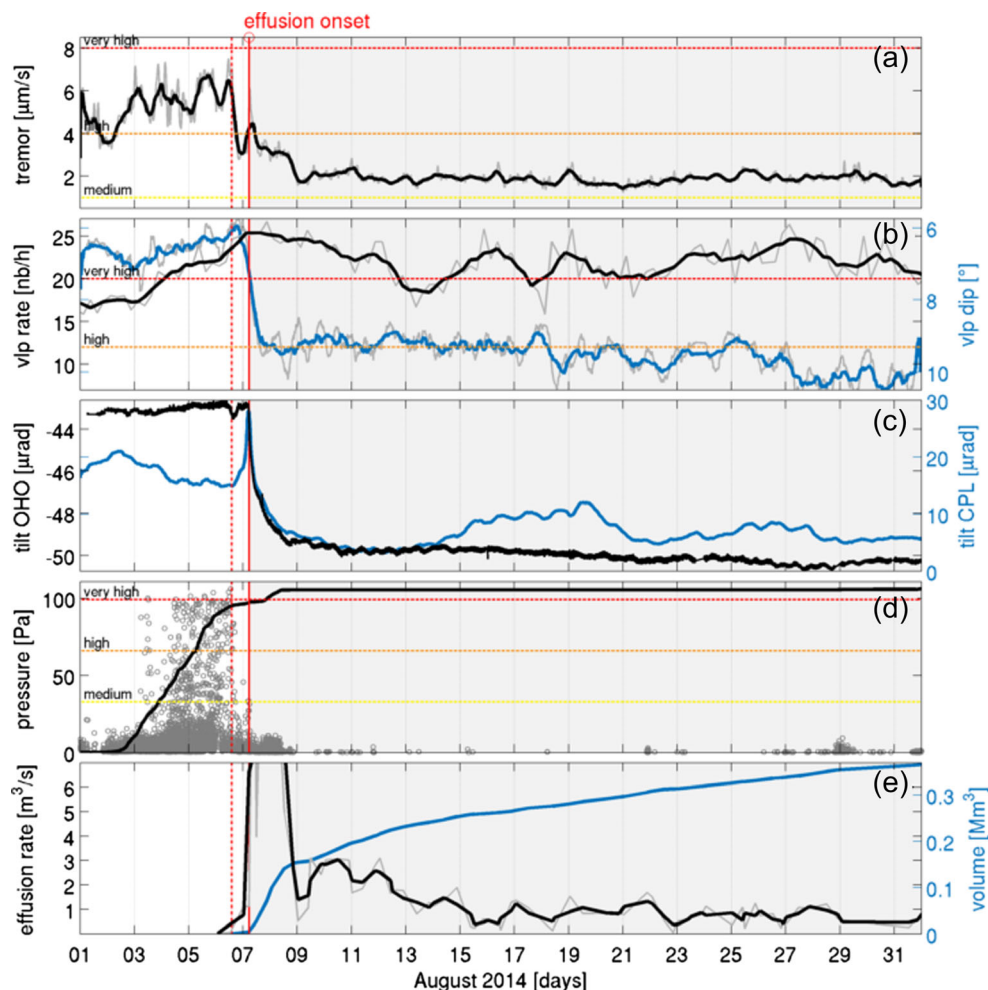
216 The opening of the new effusive vent was associated
 217 with a peak in the seismic tremor (Fig. 4(a)) which was
 218 not accompanied by an increase in infrasound activity,
 219 indicating that the seismic source was not coupled with
 220 the atmosphere and most probably related to the migration
 221 of the magma within the dyke. The migration of the mag-
 222 ma from the summit craters towards the new effusive vent
 223 probably contributed to reduction of the magma static

224 pressure working on the crater rims and possibly caused
 225 their instability which culminated with the rockfall on
 226 August 6.

Effusive phase: magma drainage 227

228 Following the vent opening, volcanic activity and geophysical
 229 parameters changed drastically, reflecting the shift from the
 230 explosive to the effusive regime. Effusive rates estimated from
 231 the analysis of MODIS thermal images shows a peak of
 232 $>20 \text{ m}^3/\text{s}$, resulting in $\sim 1.6 \times 10^6 \text{ m}^3$ of lava emitted in the
 233 first 2 days (Fig. 5(e)). During this phase, all tiltmeters record-
 234 ed a large and rapid ground deflation ($\sim 7 \mu\text{rad}$ in 48 h at the
 235 OHO station and $\sim 26 \mu\text{rad}$ at the CPL station; black and blue
 236 curves in Fig. 5(c), respectively). As the explosive activity at
 237 the summit craters ceased, the tremor amplitude dropped, and
 238 both infrasonic and thermal transients were not recorded any-
 239 more. In addition, while the rate and amplitude of VLP seismic
 240 activity remained high (Fig. 5(b), black curve), the VLP
 241 polarization dip angle increased by approximately 3° with
 242 respect to pre-effusive condition, indicating the deepening of
 243 the VLP source depth (Fig. 5(b), blue curve).

Fig. 5 Evolution of the geophysical parameters following the onset of effusion. The parameters show drastic changes following the new vent's opening: *a* drop of seismic tremor amplitude, *b* deepening of VLP seismicity yet very high VLP rate, *c* exponential ground deflation, *d* decrease and cessation of infrasonic activity, and *e* exponential decay of the lava effusion rate. The solid red bar indicates the time when the new vent opened (August 7, 2014 at 05:00 GMT), preceded nearly 15 h before (dashed vertical red bar) by the collapse of a portion of the NE1 crater and the onset of a small lava flow



244 From August 9 (3 days after the eruption onset) onwards,
 245 activity and geophysical parameters remained stable: low
 246 tremor amplitude, no infrasonic activity, no thermal signals
 247 linked to the explosive activity, and a sustained VLP rate yet
 248 with a deep source location. The effusion rate estimated from
 249 MODIS images showed an exponential decrease during the
 250 first month, reaching steady values of 0.2–0.4 m³/s from mid-
 251 September. The camera pointing at the effusive vent showed
 252 that it remained stable at ~670 m a.s.l. until the end of the
 253 eruption, which finally ceased on November 22, 2014.

254 The exponential decreasing trends of tilt, effusion rate, and
 255 VLP dip during the first 48 h suggest the rapid drainage of a
 256 shallow reservoir, which is consistent with the progressive
 257 internal collapse of the craters reported from field observa-
 258 tions and thermal infrared camera surveys (Fig. 6).

259 Model of magma discharge

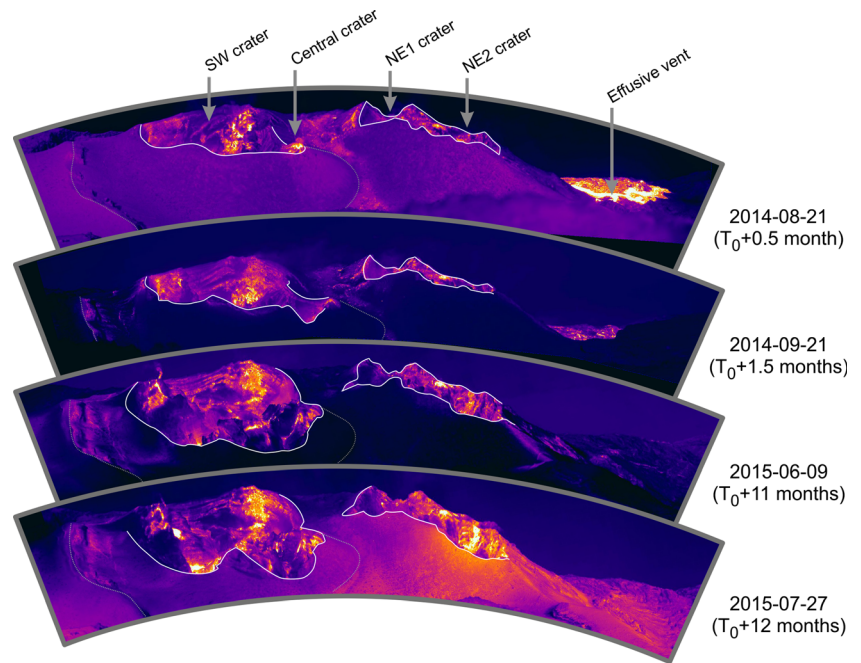
260 We explain all the recorded geophysical parameters by using a
 261 dynamical model based on the migration of the magma col-
 262 umn within the shallow conduits. We assume that during the

263 months preceding the effusive onset, magma accumulated in a 263
 264 shallow reservoir, which was then suddenly drained out from 264
 265 the newly opened effusive vent. The reservoir drainage pro- 265
 266 cess can be modeled as the discharge of a cylindrical conduit 266
 267 confined between the new effusive vent and the crater terrace 267
 268 (Ripepe et al. 2015). If the magma is flowing out the vent 268
 269 through a dyke as a Poiseuille flow, neglecting the effect of 269
 270 the atmospheric pressure, the velocity ($u(t)$) at which lava is 270
 271 flowing out the vent can be expressed as 271

$$u(t) = \frac{a^2}{4\eta L} P_h(t) \quad (1)$$

274 where a is the effusive vent radius, η is the magma viscosity, 274
 275 and L is the dyke length. In this case, the peak pressure at the 275
 276 vent (P_h) is controlled by the change in the magmastatic pres- 276
 277 sure gradient in the reservoir, such as $P_h(t) = \rho g h(t)(1 - \Phi)$, 277
 278 where $h(t)$ is the magma level height above the vent, ρ is the 278
 279 dense rock equivalent (DRE) magma density, Φ is the magma 279
 280 vesicularity, and g is the acceleration due to gravity. The effu- 280
 281 sion rate of the lava drained out the reservoir ($Q_R(t)$) can be 281
 282

Fig. 6 Thermal infrared camera surveys during the months following the onset of effusion (T_0), showing a progressive internal collapse of the crater walls. (Images were recorded with a FLIR SC660 camera)



Q10

283 expressed as

$$286 \quad Q_R(t) = \pi a^2 u(t) = (1-\Phi) \frac{\pi a^4}{8\eta L} \rho g h(t) \quad (2)$$

287 which explains that when the lava is drained out the vent,
 288 the magma level ($h(t)$) in the reservoir will progressively
 289 drop, from the maximum reservoir height (h_0) to the ele-
 290 vation of the effusive vent (670 m a.s.l.). However, the
 291 discharge of the reservoir is likely buffered by the magma
 292 supply rate from depth (Q_D), which is continuously feed-
 293 ing the shallow reservoir also during the eruption. The
 294 total lava output rate (Q_T) at the vent is therefore con-
 295 trolled by the balance between the rapid drainage of the
 296 shallow reservoir (Q_R) and the constant deep magma input
 297 rate (Q_D), such as $Q_T(t) = Q_R(t) + Q_D(t)$.

298 This model was first proposed to explain the 2007 lava
 299 flow at Stromboli (Ripepe et al. 2015) and has recently been
 300 applied also to the 2014 eruption (Zakšek et al. 2015). In
 301 agreement with previous papers, we thus used magma physi-
 302 cal parameters typical for Stromboli, such as viscosity
 303 ($\eta = 10^4$ Pa) (Métrich et al. 2001) and DRE density
 304 ($\rho = 2950$ kg/m³) (Pioli et al. 2014), whereas parameters like
 305 the radius of the effusive vent ($a = 2$ m) was measured from
 306 the thermal images. Considering magma vesicularity (Φ) can
 307 vary between 0 and 0.45 (Landi et al. 2009), we found that the
 308 best fit between the modeled and the measured data is reached
 309 for a dyke length (L) of 30 m and the reservoir height (h_0) of
 310 47 ± 10 m.

311 If no magma is considered to be supplied from depth
 312 ($Q_D = 0$), the magma static pressure will rapidly drain all
 313 the magma out of the shallow reservoir in a few days

(Ripepe et al. 2015) and the model will fail to explain
 the long-lasting effusion rate and the volume of the ex-
 truded magma (Fig. 7b, dashed blue line). Therefore, a
 magma supply rate from depth has to be considered to
 recharge the shallow reservoir also during the effusive
 magma discharge phase. While for the 2007 eruption a
 constant $Q_D = 0.7$ m³/s has been successfully used to fit
 both effusion rate and discharged magma volume (Ripepe
 et al. 2015), for the 2014 eruption, the constant
 $Q_D = 0.4$ m³/s well explains the effusion rate (Zakšek
 et al. 2015) but fails to reproduce the 107-day-long vol-
 ume of discharged magma (Fig. 7, solid blue line).

We found that the linear decrease of Q_D from 0.6–0.85 m³/s
 at the onset of the eruption to 0.3 m³/s at the end of the erup-
 tion (typical during the ordinary explosive activity at
 Stromboli, e.g., Ripepe et al. 2005; Burton et al. 2007) best
 fits both the effusion rate and discharged volume trends mea-
 sured by the MODIS sensor (Fig. 7a, b, respectively, red
 curves).

The rapid drainage process modeled by the gravity-
 induced discharge of the shallow reservoir is also in
 agreement with both the rapid deepening of the VLP seis-
 mic source and the rapid ground deflation observed dur-
 ing the first days (Fig. 8a, b). In particular, if we assume
 that the effusive eruption results from the emptying of a
 shallow reservoir located above the effusive vent, this
 model provides a simple explanation to the deepening rate
 of the VLP source, which is associated with the progres-
 sive drop of the magma level in the shallow reservoir and
 with the subsequent decrease of the residual magma vol-
 ume (Fig. 8a). This also suggests that VLP seismic

314
 315
 316
 317
 318
 319
 320
 321
 322
 323
 324
 325
 326
 327
 328
 329
 330
 331
 332
 333
 334
 335
 336
 337
 338
 339
 340
 341
 342
 343
 344

/Q11

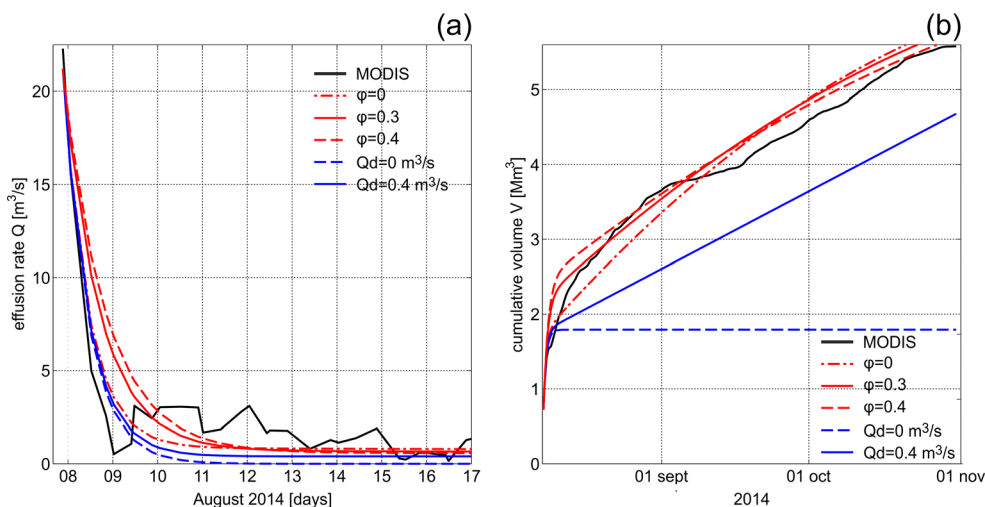


Fig. 7 Modeling of the effusion rate and volumes of lava based on the gravity-driven discharge of a shallow reservoir confined between the eruptive vent (670 m a.s.l.) and the crater terrace (770 m a.s.l.). **a** Measured and modeled effusion rate during the first 10 days following the lava onset. **b** Measured and modeled cumulative lava volume emitted during the entire effusive period. The black curves represent the measured

data (MODIS) and the red/blue curves the modeled data. Red curves consider a linearly decreasing Q_D value throughout the effusive period (with magma vesicularities of $\Phi = 0$, $\Phi = 0.3$, and $\Phi = 0.4$, respectively), while blue curves consider a constant Q_D value ($Q_D = 0 \text{ m}^3/\text{s}$, dashed blue curve; $Q_D = 0.4 \text{ m}^3/\text{s}$, solid blue curve)

345 activity is likely generated at the top of the magma col- 357
 346 umn. Moreover, the emptying of the shallow reservoir 358
 347 induces a decompression of the system, which explains 359
 348 why the modeled effusion rate fits the observed ground 360
 349 deformation rate (Fig. 8b). This suggests a shallow posi- 361
 350 tion of the deformation source (likely above 500 m a.s.l.,
 351 e.g., Marchetti et al. 2009; Ripepe et al. 2015) rather than
 352 the deep source (>1 km below sea level, e.g., Bonaccorso
 353 1998). Finally, the progressive decrease of the input rate
 354 during the months following the effusive onset induces a
 355 decrease of the magma pressure at the vent, which, as
 356 already observed for the 2002–2003 eruption (Ripepe

et al. 2005), ultimately results in the vent closure only
 when the magma input rate decreases back to the station-
 ary $0.3 \text{ m}^3/\text{s}$ value of magma input rate which character-
 izes the ordinary explosive activity.

Discussion

Measurements of the SO_2 gas flux indicate that the shallow
 system sustaining the Strombolian activity is continuously fed
 by a deep magma supply rate of $0.1\text{--}0.5 \text{ m}^3/\text{s}$ (e.g., Burton
 et al. 2009). However, gas/mass fraction shows that only

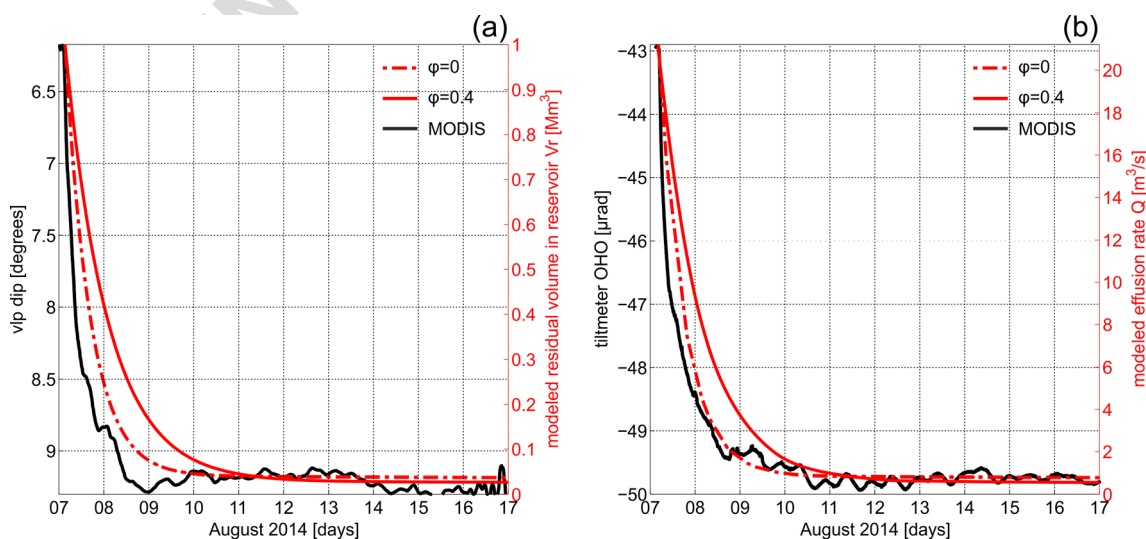


Fig. 8 a Comparison between the measured deepening of the VLP seismicity (black) and the modeled decay of magma volume in the reservoir following the vent opening (red). **b** Comparison between the

ground deflation measured at the OHO tiltmeter (black) and the modeled effusion rate following the vent opening (red). The dashed red curves take account for magma vesicularity ($\Phi = 0$ and $\Phi = 0.4$, respectively)

366 ~10 % of the magma is ejected during the explosive activity, 399
 367 suggesting that almost 90 % of the magma supplied remain in 400
 368 the feeding conduits (Allard et al. 1994; Harris and Stevenson 401
 369 1997; Allard et al. 2008). This degassed magma is inducing 402
 370 density convection conduit dynamics (Stevenson and Blake 403
 371 1998; Landi et al. 2004), keeping the feeding system at equi- 404
 372 librium. When the magma input rate increases, this equilibri- 405
 373 um is lost. During such periods of higher magma recharge, the 406
 374 excess of magma confined within the edifice is exclusively 407
 375 dissipated throughout the explosive activity at the summit 408
 376 craters, which is however not able to evacuate the larger vol- 409
 377 umes of new magma supplied. The increased magma static 410
 378 pressure associated with the increased level of magma in the 411
 379 conduit is likely to induce magma migration into dykes (or 412
 380 sills) and eventually leads to the opening of effusive vents on 413
 381 the flank of the edifice. The geophysical data collected during 414
 382 the recent 2014 eruption is consistent with such scenario, i.e., 415
 383 a process of magma recharge and drainage of a shallow 416
 384 reservoir. 417

385 The higher supply of magma to the shallow reservoir is 418
 386 recorded months before the effusive onset and is responsible 419
 387 for the progressive transition towards a higher explosive re- 420
 388 gime (Fig. 9) with respect to the usual Strombolian activity. 421
 389 Besides lava overflows, the main geophysical pieces of evi- 422
 390 dence of the response of the shallow conduit system to this 423
 391 higher magma supply rate are (1) the increasing number of 424
 392 eruptive vents, (2) the increased rate of explosive activity re- 425
 393 corded by thermal sensors, (3) the increase of tremor ampli- 426
 394 tude and infrasonic pressure, and (4) the migration of the VLP 427
 395 seismic source towards the surface. The effusive onset, typi- 428
 396 cally lasting <24 h, is characterized by the lateral propaga- 429
 397 tion of shallow dykes, evidenced by both (1) localized ground 430
 398 inflation and (2) increased landslide activity. When the dyke 431

reaches the surface, it opens a new effusive vent from which 399
 lava is drained out of the shallow conduit system. The shift 400
 from explosive to effusive regime is then recorded as (1) the 401
 absence of thermal and infrasound transients, (2) the decrease 402
 of tremor amplitude, (3) the large ground deflation, and (4) the 403
 deepening of the source of VLP seismicity. The direct conse- 404
 quence of the transition to the effusive regime is the progres- 405
 sive collapse of the crater terrace, revealing the gravitational 406
 instability induced by the large amount of drained magma 407
 from the shallow portion of the conduit system. 408

409 These observations were modeled as the consequence of 410
 the gravity-driven discharge process of a shallow reservoir 411
 (Ripepe et al. 2015). The good fit between the modeled effu- 412
 sion rate and the one measured from satellite (Fig. 7) suggests 413
 that the largest part of the lava emplaced during the first days 414
 was already stored in a shallow reservoir confined above the 415
 effusive vent. This model also explains the rapid deepening of 416
 the VLP seismic source (Fig. 8a) and the ground deflation 417
 measured by the tiltmeters (Fig. 8b). 418

419 This gravity-driven process proposed to explain small 420
 lateral eruptions at Stromboli (Ripepe et al. 2015; Zakšek 421
 et al. 2015) has been used to describe and model geophys- 422
 ical observations of other mafic volcanic larger-scale 423
 eruptions. At the Kīlauea Volcano, the lateral eruption rate 424
 from Kīlauea's east rift zone has shown to scale with 425
 changes in the Halema'uma'u lava lake level and summit 426
 deformation (Patrick et al. 2015). At the Nyamuragira 427
 Volcano, the collapse of the summit pit crater was associ- 428
 ated with waning lateral effusion rates (Coppola et al. 429
 2016a), and more recently, the large effusive eruption at 430
 the Bárðarbunga Volcano has shown lateral effusion rate 431
 to correlate with caldera subsidence (Coppola et al. 2016b; Gudmundsson et al. 2016). These similarities

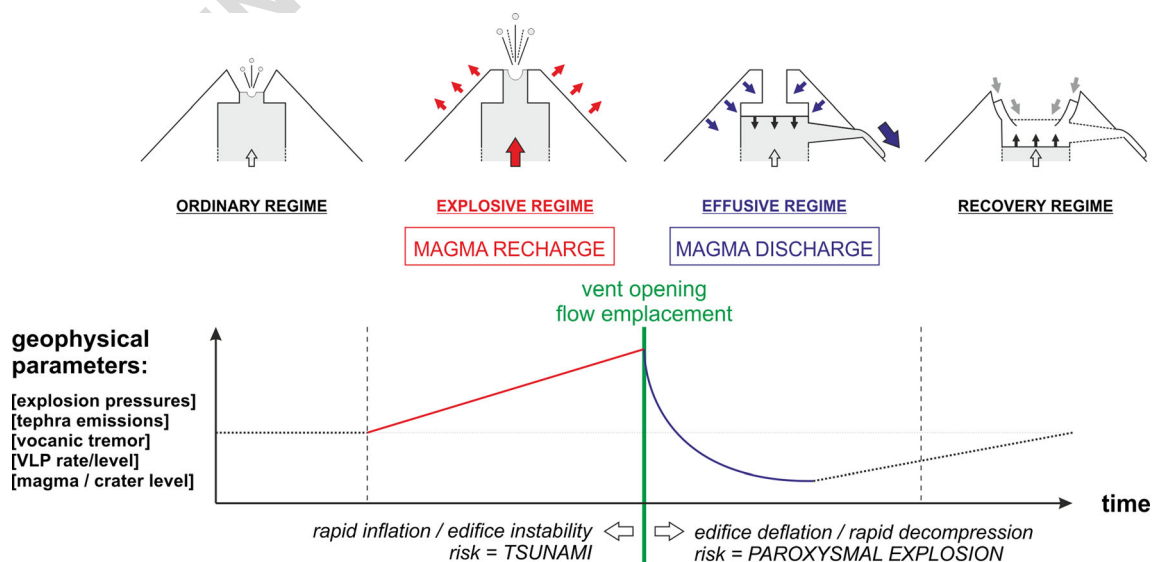


Fig. 9 Interpretive sketch of the magma recharge and discharge dynamics, suggested from geophysical observations, and implications for associated hazards

432 suggest that lateral magma effusion rates are controlled by
433 variations in the magma column level and that tracking
434 this level using geophysical parameters such as the VLP
435 seismicity, the lava lake level, or the caldera subsidence
436 becomes fundamental for monitoring effusive eruption on
437 a volcano's flank.

438 Hazard implications

439 During the pre-eruptive (magma recharging) phase, in re-
440 sponse to the higher magma supply, the edifice slowly de-
441 forms (Fig. 9). Although clear inflation trends are difficult to
442 identify (probably because inflation is too slow and thus easily
443 masked by seasonal ground deformation and earth tides), the
444 mean rate of rockfall events usually increases in the late stage
445 and immediately before opening of the effusive vent,
446 reflecting a general flank instability (Marchetti et al. 2009;
447 Di Traglia et al. 2014). As previously observed during the
448 onset of the 2002–2003 eruptive crisis, the inflation may lead
449 to large landslides triggering tsunami waves that may affect
450 the coast of Sicily and Calabria (Tinti et al. 2006; Chiocci et al.
451 2008).

452 The supply of magma at increased rate is also responsible
453 for increased explosive activity, and the risk of new vent open-
454 ing becomes very high. Interestingly, the effusive vents
455 opened during the effusive crisis of 2003, 2007, and 2014
456 were all located northeast of the SW–NE crater alignment.
457 This crater alignment is thought to result from the orientation
458 of the feeding dike, which follows well-known regional tec-
459 tonic alignments (Rosi 1980; Hornig-Kjarsgaard et al. 1993;
460 Keller et al. 1993; Tibaldi 2001). The fact that new effusive
461 vents systematically open to the northeast is likely the result of
462 a relatively shallow structural factor: the southwest border of
463 the crater terrace is confined by an old collapse scar acting as a
464 rigid boundary, whereas the northeast border is composed of
465 loose pyroclastic material ejected from the NE crater sector
466 (Tibaldi 2001).

467 Once the eruptive vent opens, the entire system depressur-
468 izes following the effusion rate, and there is overall deflation
469 of the edifice. In this phase, the main hazard is thus no longer
470 the flank instability and potential generation of tsunamis, but
471 processes taking place during the recovery of equilibrium in
472 the magmatic system, in response to the drainage of the up-
473 permost portion of the edifice. During the effusive crises in
474 2003 and 2007, violent paroxysmal eruptions occurred during
475 this recovery, ejecting blocks which fell at an elevation of
476 450 m a.s.l., 1 km from the craters on the northeastern slope,
477 and as far as the village of Ginostra (~2 km from the crater
478 area) on the western slope (Rosi et al. 2006; Pistolesi et al.
479 2011). These events are commonly explained as resulting
480 from the rapid ascent of parcels of a deep-seated (7–9 km),
481 gas-rich low-porphyricity (LP) magma which eventually

interacts with a shallow (2–3 km), high-porphyricity (HP) 482
reservoir (Bertagnini et al. 2003; Métrich et al. 2009). 483
Calvari et al. (2011) suggested that during effusive eruptions, 484
the removal of a large volume of magma ($\sim 6.5 \times 10^6 \text{ m}^3$ of 485
16–32 vol% vesicular lava) from the shallow reservoir can be 486
responsible for paroxysmal eruptions. Following the 2014 487
eruption, $\sim 5.5 \times 10^6 \text{ m}^3$ of lava were emplaced in 107 days 488
but no paroxysmal eruption occurred. Although the critical 489
value suggested by Calvari et al. (2011) was not reached, the 490
longer duration over which the total volume was emplaced in 491
2014 suggests that the controlling factor of such paroxysms 492
may be the rate at which magma is drained out rather than the 493
total volume of magma erupted. Based on this observation, we 494
infer that decompression induced by the rapid removal of 495
magma from the conduit system (that is large volumes in short 496
time) could be responsible for triggering violent explosive 497
paroxysms at Stromboli. 498

Acknowledgments We wish to thank Salvatore Zaia and Vivian 499
Anceschi for their continuous support at the Centro Operativo Avanzato 500
of Stromboli (COA). This work was supported by the Italian Civil 501
Protection in the framework of the DEVNET project. The paper has been 502
improved by constructive comments by the Associate Editor Matthew 503
Patrick, the reviewer Matt Haney, and an anonymous reviewer, all of 504
whom we wish to thank. 505

References 506 Q12

- Allard P, Carbonnelle J, Métrich N, Loyer H, Zettwoog P (1994) Sulphur 508
output and magma degassing budget of Stromboli Volcano. *Nature* 509
368:326–330. doi:10.1038/368326a0 510
- Allard P, Aiuppa A, Burton M, Caltabiano T, Federico C, Salerno G, La 511
Spina A (2008) Crater gas emissions and the magma feeding system 512
of Stromboli Volcano. In: Calvari S, Inguaggiato S, Ripepe M., Rosi 513
M. (ed) *The Stromboli Volcano: an integrated study of the 2002–* 514
2003 eruption. AGU, Washington DC, Geophysical Monograph 515
Series, 182:65–80. doi:10.1029/182GM07 516
- Barberi F, Rosi M, Sodi A (1993) Volcanic hazard assessment at 517
Stromboli based on review of historical data. *Acta Vulcanol* 3: 518
173–187 519
- Barberi F, Civetta L, Rosi M, Scandone R (2009) Chronology of the 2007 520
eruption of Stromboli and the activity of the Scientific Synthesis 521
Group. *J Volcanol Geotherm Res* 182(3–4):123–130. doi:10.1016 522
/j.jvolgeores.2008.09.019 523
- Bertagnini A, Métrich N, Landi P, Rosi M (2003) Stromboli Volcano 524
(Aeolian Archipelago, Italy): an open window on the deep-feeding 525
system of a steady state basaltic volcano. *J Geophys Res* 108-7:1– 526
15. doi:10.1029/2002JB002146 527
- Bonaccorso S (1998) Evidence of a dyke-sheet intrusion at Stromboli 528
Volcano inferred through continuous tilt. *Geophys Res Lett* 529
25(22):4225–4228. doi:10.1029/1998GL900115 530
- Burton M, Allard P, Mure F, La Spina A (2007) Magmatic gas composi- 531
tion reveals the source depth of slug-driven Strombolian explosive 532
activity. *Science* 317(5835):227–230. doi:10.1126/science.1141900 533
- Burton M, Caltabiano I, Mure E, Salerno G, Randazzo D (2009) SO₂ flux 534
from Stromboli during the 2007 eruption: results from the FLAME 535
network and traverse measurements. *J Volcanol Geotherm Res* 536
182(3–4):214–220. doi:10.1016/j.jvolgeores.2008.11.025 537

- 538 Calvari S, Spampinato L, Lodato L, Harris AJL, Patrick MR, Dehn J, 602Q13
 539 Burton MR, Andronico D (2005) Chronology and complex volcanic 603
 540 processes during the 2002–2003 flank eruption at Stromboli 604
 541 Volcano (Italy) reconstructed from direct observations and surveys 605
 542 with a hand-held thermal camera. *J Geophys Res* 110:B02201. 606
 543 doi:10.1029/2004JB003129 607
- 544 Calvari S, Lodato L, Steffke A, Cristaldi A, Harris AJL, Spampinato L, 608
 545 Boschi E (2010) The 2007 Stromboli flank eruption: event chronol- 609
 546 ogy and effusion rates using thermal infrared data. *J Geophys Res* 610
 547 115(B04201). doi: 10.1029/2009JB006478 611
- 548 Calvari S, Spampinato L, Bonaccorso A, Oppenheimer C, Rivalta E, 612
 549 Boschi E (2011) Lava effusion—a slow fuse for paroxysms at 613
 550 Stromboli Volcano? *Earth Planet Sci Lett* 301(1–2):317–323. 614
 551 doi:10.1016/j.epsl.2010.11.015 615
- 552 Chaussard E, Amelung F, Aoki Y (2013) Characterization of open and 616
 553 closed volcanic systems in Indonesia and Mexico using InSAR time 617
 554 series. *J Geophys Res Solid Earth* 118:1–13. doi:10.1002/ 618
 555 /jgrb.50288 619
- 556 Chiocci FL, Romagnoli C, Tommasi P, Bosman A (2008) The Stromboli 620
 557 2002 tsunamigenic submarine slide: characteristics and possible fail- 621
 558 ure mechanisms. *J Geophys Res Solid Earth* 113(10):B10102. 622
 559 doi:10.1029/2007JB005172 623
- 560 Coppola D, Laiolo M, Piscopo D, Cigolini C (2013) Rheological control 624
 561 on the radiant density of active lava flows and domes. *J Volcanol 625*
 562 *Geotherm Res* 249:39–48. doi:10.1016/j.jvolgeores.2012.09.005 626
- 563 Coppola D, Laiolo M, Cigolini C, Delle Donne D, Ripepe M (2015) 627
 564 Enhanced volcanic hot-spot detection using MODIS IR data: results 628
 565 from the MIROVA system. In: Harris AJL, De Groeve T, Garel F, 629
 566 Carn SA (ed), *Detecting, modelling and responding to effusive eruptions*. 630
 567 Geological Society, London, Special Publications, 426. 631
 568 doi:10.1144/SP426.5 632
- 569 Coppola D, Campion R, Laiolo M, Cuoco E, Balagizi C, Ripepe M, 633
 570 Cigolini C, Tedesco D (2016a) Birth of a lava lake: Nyamulagira 634
 571 Volcano 2011–2015. *Bull Volcanol* 78(3):1–13. doi:10.1007/ 635
 572 /s00445-016-1014-7 636
- 573 Coppola D, Laiolo M, Cigolini C, Barsotti S, Jónasdóttir E, Ripepe M 637
 574 (2016b) Effusion rates, volumes and emplacement style using 638
 575 MODIS MIR data: the 2014–15 Holuhraun eruption (Bárðarbunga, 639
 576 Iceland) tracked by MIROVA. *EGU General Assembly 2016 18:* 640
 577 *EGU2016–16308* 641
- 578 De Fino M, La Volpe L, Falsaperla S, Frazzetta G, Neri G, Francalanci L, 642
 579 Rosi M, Sbrana A (1988) The Stromboli eruption of December 6, 643
 580 1985 - April 15, 1986: volcanological, petrological and seismologi- 644
 581 cal data. *Rendiconti della Società Italiana di Mineralogia e 645*
 582 *Petrologia* 43:1021–1038 646
- 583 Delle Donne D, Ripepe M (2012) High-frame rate thermal imagery of 647
 584 strombolian explosions: implications for explosive and infrasonic 648
 585 source dynamics. *J Geophys Res Solid Earth* 117(9):B09206. 649
 586 doi:10.1029/2011JB008987 650
- 587 Di Traglia F, Nolesini T, Intrieri E, Mugnai F, Leva D, Rosi M, Casagli N 651
 588 (2014) Review of ten years of volcano deformations recorded by the 652
 589 ground-based InSAR monitoring system at Stromboli Volcano: a 653
 590 tool to mitigate volcano flank dynamics and intense volcanic activ- 654
 591 ity. *Earth-Sci Rev* 139:317–335. doi:10.1007/s00445-013-0786-2 655
- 592 Gudmundsson MT et al. (2016) Gradual caldera collapse at Bárðarbunga 656
 593 volcano, Iceland, regulated by lateral magma outflow. *Science* 353 657
 594 (6296). doi:10.1126/science.aaf8988 658
- 595 Harris AJL, Stevenson DS (1997) Magma budgets and steady-state activ- 659
 596 ity of Vulcano and Stromboli volcanoes. *Geophys Res Lett* 24: 660
 597 1043–1046. doi:10.1029/97GL00861 661
- 598 Hornig-Kjarsgaard I, Keller J, Koberski U, Stadlbauer E, Francalanci L, 662
 599 Lenhart R (1993) Geology, stratigraphy and volcanological evolu- 663
 600 tion of the island of Stromboli, Aeolian Arc, Italy. *Acta Vulcanol* 3: 664
 601 21–68 665
- Istituto Nazionale di Geofisica e Vulcanologia (INGV) – Centro 602Q13
 Nazionale Terremoti. Online earthquake database available at: 603
<http://cnt.rm.ingv.it>. 604
- Keller J, Hornig-Kjarsgaard I, Koberski U, Stadlbauer E, Francalanci L, 605
 Lenhart R (1993) Geological map of the island of Stromboli. *Acta 606*
Vulcanologica 607
- Landi P, Métrich MN, Bertagnini A, Rosi M (2004) Dynamics of magma 608
 mixing and degassing recorded in plagioclase at Stromboli (Aeolian 609
 Archipelago, Italy). *Contrib Mineral Petrol* 147:213–227. 610
 doi:10.1007/s00410-004-0555-5 611
- Landi P, Corsaro RA, Francalanci L, Civetta L, Miraglia L, Pompilio M, 612
 Tesoro R (2009) Magma dynamics during the 2007 Stromboli erup- 613
 tion (Aeolian Islands, Italy): mineralogical, geochemical and isoto- 614
 pic data. *J Volcanol Geotherm Res* 182(3–4):255–268. doi:10.1016 615
 /j.jvolgeores.2008.11.010 616
- Marchetti E, Ripepe M (2005) Stability of the seismic source during 617
 effusive and explosive activity at Stromboli Volcano. *Geophys Res 618*
 Lett 32:L03307. doi:10.1029/2004GL021406 619
- Marchetti E, Genco R, Ripepe M (2009) Ground deformation and seis- 620
 micity related to the propagation and drainage of the dyke feeding 621
 system during the 2007 effusive eruption at Stromboli Volcano 622
 (Italy). *J Volcanol Geotherm Res* 182(3–4):155–161. doi:10.1016 623
 /j.jvolgeores.2008.11.016 624
- Marsella M, Baldi P, Coltelli M, Fabris M (2011) The morphological 625
 evolution of the Sciarra del Fuoco since 1868: reconstructing the 626
 effusive activity at Stromboli Volcano. *Bull Volcanol* 74:231–248. 627
 doi:10.1007/s00445-011-0516-6 628
- Métrich N, Bertagnini A, Landi P, Rosi M (2001) Crystallization driven 629
 by decompression and water loss at Stromboli Volcano (Aeolian 630
 Islands, Italy). *J Petrol* 42(8):1471–1490. doi:10.1093 631
 /petrology/42.8.1471 632
- Métrich N, Bertagnini A, Di Muro A (2009) Conditions of magma stor- 633
 age, degassing and ascent at Stromboli: new insights into the volca- 634
 no plumbing system with inferences on the eruptive dynamics. *J 635*
Petrol 51(3):603–626. doi:10.1093/petrology/egp083 636
- Patrick MR, Anderson KR, Poland MP, Orr T, Swanson DA (2015) Lava 637
 lake level as a gauge of magma reservoir pressure and eruptive 638
 hazard. *Geology* 43:831–834. doi:10.1130/G36896.1 639
- Pioli L, Pistolesi M, Rosi M (2014) Transient explosions at open-vent 640
 volcanoes: the case of Stromboli (Italy). *Geology* 42(10):863–866. 641
 doi:10.1130/G35844.1 642
- Pistolesi M, Delle Donne D, Pioli L, Rosi M, Ripepe M (2011) The 15 643
 March 2007 explosive crisis at Stromboli Volcano, Italy: assessing 644
 physical parameters through a multidisciplinary approach. *J 645*
Geophys Res 116:B12206. doi:10.1029/2011JB008527 646
- Ripepe M, Marchetti E, Poggi P, Harris AJL, Fiaschi A, Olivieri G (2004) 647
 Seismic, acoustic, and thermal network monitors the 2003 eruption 648
 of Stromboli Volcano. *Eos* 85(35):329–336 649
- Ripepe M, Marchetti E, Olivieri G, Harris A, Dehn J, Burton M, 650
 Caltabiano T, Salerno G (2005) Effusive to explosive transition dur- 651
 ing the 2003 eruption of Stromboli Volcano. *Geology* 33(5):341– 652
 344. doi:10.1130/G21173.1 653
- Ripepe M, Marchetti E, Olivieri G (2007) Infrasonic monitoring at 654
 Stromboli Volcano during the 2003 effusive eruption: insights 655
 on the explosive and degassing process of an open conduit 656
 system. *J Geophys Res* 112:B09207. doi:10.1029/2006 657
 JB004613 658
- Ripepe M, Delle Donne D, Lacanna G, Marchetti E, Olivieri G (2009) 659
 The onset of the 2007 Stromboli effusive eruption recorded by an 660
 integrated geophysical network. *J Volcanol Geotherm Res* 182(3–4): 661
 131–136. doi:10.1016/j.jvolgeores.2009.02.011 662
- Ripepe M, Delle Donne D, Genco R, Maggio G, Pistolesi M, Marchetti E, 663
 Lacanna G, Olivieri G, Poggi P (2015) Volcano seismicity and 664
 ground deformation unveil the gravity-driven magma discharge dy- 665
 namics of a volcanic eruption. *Nat Commun* 6:6998. doi:10.1038 666
 /ncomms7998 667

- 668 Rosi M (1980) The island of Stromboli. *Rend Soc It Min Pet* 36:345–368
- 669 Rosi M, Bertagnini A, Landi P (2000) Onset of the persistent activity at
670 Stromboli Volcano (Italy). *Bull Volcanol* 62(4–5):294–300.
671 doi:[10.1007/s004450000098](https://doi.org/10.1007/s004450000098)
- 672 Rosi M, Bertagnini A, Harris AJL, Pioli L, Pistolesi M, Ripepe M (2006)
673 A case history of paroxysmal explosion at Stromboli: timing and
674 dynamics of the April 5, 2003 event. *Earth Planet Sci Lett* 243:594–
675 606
- 676 Rosi M, Pistolesi M, Bertagnini A, Landi P, Pompilio M, Di Roberto A
677 (2013) Stromboli volcano, Aeolian Islands (Italy): present eruptive
678 activity and hazards. In: Lucchi F, Peccerillo A, Keller J, Tranne CA,
679 Rossi PL (ed), *The Aeolian Islands volcanoes*, Geological Society,
680 London, *Memoirs*, 37:473–490. doi:[10.1144/M37.14](https://doi.org/10.1144/M37.14)
- 695
- Stevenson DS, Blake S (1998) Modelling the dynamics and thermody- 681
namics of volcanic degassing. *Bull Volcanol* 60:307–317. 682
doi:[10.1007/s004450050234](https://doi.org/10.1007/s004450050234) 683
- Tibaldi A (2001) Multiple sector collapses at Stromboli Volcano, Italy: 684
how they work. *Bull Volcanol* 63:112–125. doi:[10.1007/s004450100129](https://doi.org/10.1007/s004450100129) 685
686
- Tinti S, Maramai A, Armigliato A, Graziani L, Manucci A, Pagnoni 687
G, Zaniboni F (2006) Observations of physical effects from 688
tsunamis of December 30, 2002 at Stromboli Volcano, 689
Southern Italy. *Bull Volcanol* 68:450–461. doi:[10.1007/s00445-005-0021-x](https://doi.org/10.1007/s00445-005-0021-x) 690
691
- Zakšek K, Hort M, Lorenz E (2015) Satellite and ground based thermal 692
observation of the 2014 effusive eruption at Stromboli Volcano. 693
Remote Sens 7:17190–17211. doi:[10.3390/rs71215876](https://doi.org/10.3390/rs71215876) 694

UNCORRECTED PROOF

AUTHOR QUERIES

AUTHOR PLEASE ANSWER ALL QUERIES.

- Q1. Please check the captured email address of author “Sebastien Valade” if correct.
- Q2. “Sebastien Valade” has been set as the corresponding author. Please check and advise if correct.
- Q3. Please check the captured affiliations if presented correctly.
- Q4. Keywords are required. The following are suggested: Magma, Open-conduit system, and Volcano. Please check if appropriate.
- Q5. The unit of measure “Mm³” was changed to “cubic megameter.” Please check if correct.
- Q6. Quotation marks, which are not used to indicate uncommon or unusual usage at first mention or that a word/phrase is being referred to as a term rather than being used in its meaning, were removed or deleted, and the terms were italicized for emphasis. Please check if appropriate.
- Q7. Please consider providing the respective expansion of the abbreviations “ROC, STR, OHO, and CPL” at the first occurrence in the text.
- Q8. Please check if changing the term “seismic VLP” in this sentence to “VLP seismic source” for consistency is correct.
- Q9. Please check if the abbreviation “a.s.l.” is defined correctly. Otherwise, please provide the correct expansion.
- Q10. Please check if insertion of the word “camera” in this sentence for completeness is correct.
- Q11. Please check if changing the term “VLP” in this sentence to “VLP seismic activity” for completeness is correct and amend if necessary.
- Q12. Reference [Istituto Nazionale di Geofisica e Vulcanologia (INGV) – C] was provided in the reference list; however, this was not mentioned or cited in the manuscript. As a rule, all references given in the list of references should be cited in the main body. Please provide its citation in the body text.
- Q13. Please provide complete bibliographic details of this reference.